MHD INSTABILITY IN ANNULAR LINEAR INDUCTION PUMPS (2D MODEL)

I.R. Kirillov, D.M. Obukhov
D.V. Efremov Institute of Electrophysical Apparatus, 196641, St. Petersburg, Russia
(kirillir@sintez.niiefa.spb.su)

Introduction. MHD instability in annular linear induction pumps (ALIP) arising in the conditions of large magnetic fields induced in liquid metal (magnetic Reynolds number $\mathrm{Rm}\, s > 1$) has been studied for some time both theoretically and experimentally [1]–[6]. The manifestation of MHD instability is a non-uniform liquid metal velocity profile, pressure and flow rate pulsations, an ALIP duct and loop pipes vibration. The 1D "jet" model [1, 2, 7, 8] showed the existence of secondary flows, allowed to estimate qualitatively the velocity profile, asymptotic values of pump pressure, showed relatively good qualitative agreement with the experiments.

2D models allowed to predict [3] the vortex secondary flows similar to the rotation stall in high-pressure axial compressors and to draw a flow picture in an ALIP [6]. Here a completely new 2D mathematical model for analysis of the flow pattern in the ALIP and its characteristics is described and tested over the experimental data.

1. Model description. The scheme of the model is shown in Fig. 1. Liquid metal flows in the x-direction in the duct of height $2b$ placed between two ferromagnetic surfaces with a current layer at one of them. The active length of the inductor is $2p_n\tau$, where $2p_n$ are the pole number, τ is the pole pitch; L_{sh} is the equivalent length of zones with account for a magnetic flux shunting at the inductor edges; x_0 is a calculation region outside the inductor.

The applied and induced magnetic fields have z-components only $\mathbf{B}_0 = \big(0, 0, B_0(x, y)\big)$, $\mathbf{b} = (0, 0, b_z(x, y))$, which are averaged over a non-magnetic gap $2\delta_0$. The velocity components $\mathbf{U} = (u, v, 0)$ are averaged over the duct height as well.

The following system of equations is to be solved:

$$-\frac{\mathrm{Rm}_e}{\omega}\frac{\partial(b_z + B_0)}{\partial t} + \frac{\partial^2 b_z}{\partial \bar{x}^2} + \frac{\partial^2 b_z}{\partial \bar{y}^2} - \mathrm{Rm}' u^* \frac{\partial(b_z + B_0)}{\partial \bar{x}^2} - \mathrm{Rm}' v^* \frac{\partial(b_z + B_0)}{\partial \bar{y}^2} = 0 \quad (1)$$

$$\frac{\partial u}{\partial t} + u\frac{\partial u}{\partial x} + v\frac{\partial u}{\partial y} = -\frac{1}{\rho}\frac{\partial p}{\partial x} + \nu_{\mathrm{eff}}\Big(\frac{\partial^2 u}{\partial x^2} + \frac{\partial^2 u}{\partial y^2}\Big) + \frac{f_x}{\rho} - \frac{c_{\mathrm{f}}}{2b} u\sqrt{u^2 + v^2}\,, \quad (2)$$

$$\frac{\partial v}{\partial t} + u\frac{\partial v}{\partial x} + v\frac{\partial v}{\partial y} = -\frac{1}{\rho}\frac{\partial p}{\partial x} + \nu_{\mathrm{eff}}\Big(\frac{\partial^2 v}{\partial x^2} + \frac{\partial^2 v}{\partial y^2}\Big) + \frac{f_y}{\rho} - \frac{c_{\mathrm{f}}}{2b} v\sqrt{u^2 + v^2}\,, \quad (3)$$

$$\frac{\partial u}{\partial x} + \frac{\partial v}{\partial y} = 0\,. \quad (4)$$

Here $\mathrm{Rm}_e = \mathrm{Rm}'(1 + \sigma_k b_k/\sigma b)$; σ_k, σ is the electric conductivity of the duct walls and liquid metal; $2b_k$ is the duct walls thickness; $\mathrm{Rm}' = \mathrm{Rm}_0(2b/2\delta')$; $\mathrm{Rm}_0 = \mu_0\sigma\omega/\alpha^2$ is the magnetic Reynolds number; $\alpha = \pi/\tau$; $2\delta' = 2\delta_0 k_\delta k_\mu$ is an equivalent non-magnetic gap, taking into account the inductor tooth-slot structure and steel magnetization; $u^* = u(\alpha/\omega)$, $v^* = v(\alpha/\omega)$, $\bar{x} = x\alpha$, $\bar{y} = y\alpha$ are the dimensionless velocities and coordinates. In Navier–Stokes equations (2), (3) the averaging of the pulsating components with Reynolds procedure and over the duct height is applied. Here ν_{eff} is the effective viscosity (a sum of laminar and turbulent viscosity), c_{f} is the local friction coefficient at the duct walls. Boundary

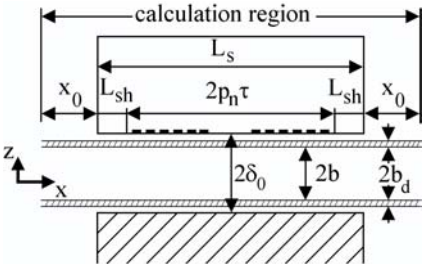

Fig. 1. Model for calculation.

conditions are the following:

$$b_z\big|_{x=0} = 0, \quad b_z\big|_{x=L} = 0, \quad b_z\big|_{y=0} = b_z\big|_{x=2\pi R}, \quad \frac{\partial b_z}{\partial y}\Big|_{y=0} = \frac{\partial b_z}{\partial y}\Big|_{y=2\pi R},$$

$$u\big|_{x=0} = u_0(y), \quad u\big|_{x=L} = u_s, \quad u\big|_{y=0} = u\big|_{y=2\pi R}, \quad \frac{\partial u}{\partial y}\Big|_{y=0} = \frac{\partial u}{\partial y}\Big|_{y=2\pi R},$$

$$v\big|_{x=0} = 0, \quad v\big|_{x=L} = 0, \quad v\big|_{y=0} = v\big|_{x=2\pi R} = 0, \quad \frac{\partial v}{\partial y}\Big|_{y=0} = \frac{\partial v}{\partial y}\Big|_{y=2\pi R},$$

where $L = L_s + 2x_0$.

The applied magnetic field was obtained as a superposition of the magnetic fields from the currents in the inductor slots as $\dot{B}_0 = \dot{B}_{0m}\mathrm{e}^{i\omega t}$, where $\dot{B}_{0m}(x, y) = \dot{B}_{0m} f_y$ is a complex amplitude. Its dependence on the y-coordinate may be taken from the experiment or, as in our case, from a model-type dependence $f(y) = 1 + 0.1\cos(y/R)$, $y \in [0, 2\pi R]$. The induced magnetic field was defined as $\dot{b}_z = b_z^{\mathrm{Re}} + ib_z^{\mathrm{Im}}$.

The electromagnetic force components were obtained with the use of electric current densities in the liquid metal. Pressure p was defined from the Poisson equation following from Eq. (2–4). Two types of the inlet velocity profile were used: uniform, $u_0 = u_s$, u_s is a mean flow rate velocity, and non-uniform, $u_0 = u_s(1 + 0.1\cos(y/R))$.

Numerical calculations were performed by the method of finite difference on a displaced uniform mesh (the points for calculating velocity were displaced with regard to the points for calculating pressure and magnetic field). Eq. (1) and Eq.(2), (3) were split applying a stabilizing correction factor. Convective terms in Eq. (2), (3) were approximated with upwind differences. The Poisson stationary equation was solved by iteration procedure and successive upper relaxation.

The following initial conditions were used: the induced magnetic field was equal to zero; the velocity components at all x were equal to that at the entrance to the calculation region.

The above described mathematical model (EMP-MHD2D) was used to analyze the electromagnetic and hydrodynamic characteristics of the electromagnetic pump ALIP-2 described in [6]. The MHD instability in this pump characterized by a non-uniform distribution of the magnetic field over azimuth and low frequency pressure pulsations was studied experimentally at a large extent [6]. The liquid metal velocity was not measured directly in this experiment, but the distribution of its x-component over the duct length and azimuth may be judged by the distribution of the magnetic field, as shown in [5].

2. Results of calculation. Numerical modeling results are presented in Figs. 2–5 for $\mathrm{Rm}' = 2.94$ and $s = 0.72$. As a result of calculations, the 2D model demonstrates two types of the liquid metal flow. For $\mathrm{Rm}'\,s$ less than some critical value $\mathrm{Rm}'\,s \approx 1.4$ for the pump tested-fully a uniform flow with $v = 0$ is realized in the whole calculation region in the absence of the applied magnetic field and inlet flow velocity non-uniformity. Low non-uniformity of the applied magnetic field results under these conditions in a low non-uniformity of the flow velocity.

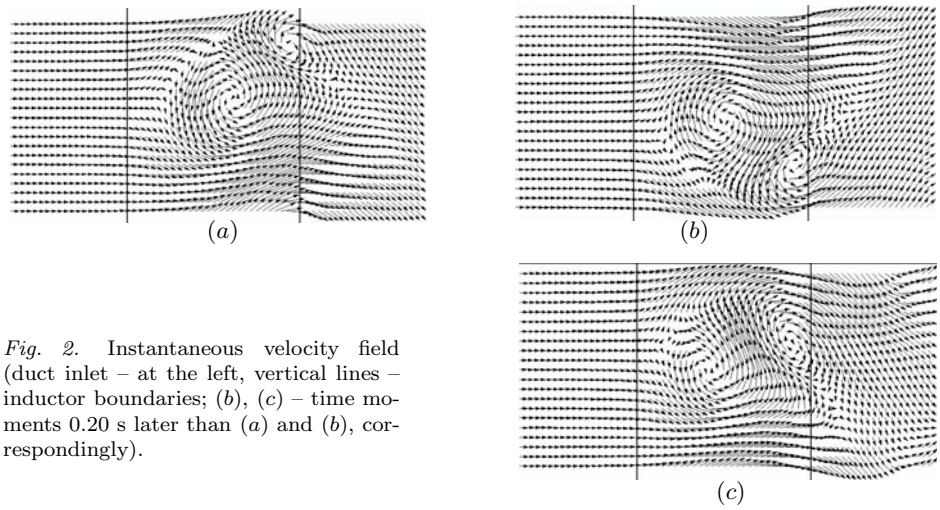

Fig. 2. Instantaneous velocity field (duct inlet – at the left, vertical lines – inductor boundaries; (*b*), (*c*) – time moments 0.20 s later than (*a*) and (*b*), correspondingly).

The pressure developed by the pump has a component pulsating in time with a double supply frequency (DSF) of the feeding current only.

At Rm′ *s* larger than this critical value, the flow is still uniform in the absence of outer non-uniformity. But in the presence of the applied magnetic field or inlet velocity non-uniformity, there exists a strong flow non-uniformity with large-scale vortices in the inductor region, which are transferred from the inlet to the outlet and in the azimuthal direction. An example of such vortices is shown in Fig. 2 for some time moments. The larger the Rm′ *s* values, the more non-uniform becomes the flow – azimuthal and longitudinal velocity components become comparable, and the azimuthal displacement of the vortices becomes large. The pump pressure in this regime contains high and low frequency pulsations (Fig. 3). The frequency spectrum of the pressure pulsations is shown in Fig. 4 and qualitatively coincides with the experimental one [6]. The flow character fits qualitatively with the calculated one in [6], though the models differ significantly.

The averaged over time calculated velocity profiles are shown in Fig. 5 for some cross-sections along the duct length. Results of calculation over the 1D model (EMP2D-JET) [8] are shown for comparison as well. The calculation results show that at $s = 0.47$ the degree of non-uniformity increases from the duct inlet to the outlet, while at $s = 0.72$ and $s = 0.78$ the non-uniformity is larger, on the one hand, and increases up to about 3/4 of the duct length and decreases further on, on the other hand. The velocity maximum values have physical sense for the 2D model, while for the 1D model they are too large. The calculation results for the averaged velocity profiles correspond qualitatively well to the experimental results on the magnetic field distribution [6].

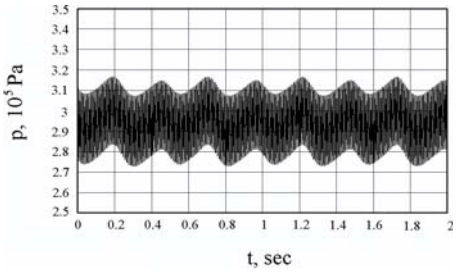

Fig. 3. Pressure developed by the pump.

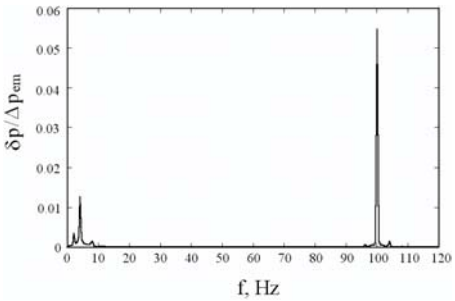

Fig. 4. Spectrum of the developed pressure.

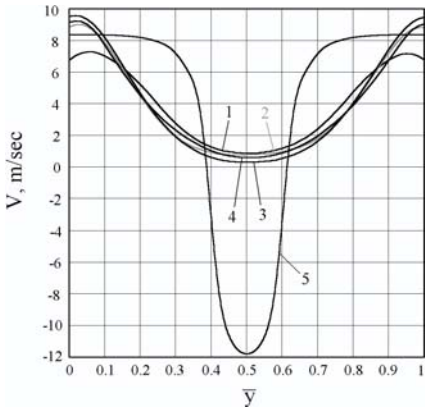

Fig. 5. Time averaged velocity profiles over azimuth (1, 2, 3 – 1/4, 1/2, 3/4 of the inductor length; 4 – inductor outlet; 5 – 1D model calculation).

The pump pressure Δp (independent on the time component) calculated over the 2-D model corresponds within 3–9% to the experimental data and is close to the results of the 1D model (see Table 1).

The amplitude of the main low frequency pulsation $\delta p_{\rm low}$ calculated over the 2D model is compared to the experimental data in Table 1; the difference may be explained partly by the fact that the model type non-uniformity of the applied magnetic field was used in the analysis, which differs from the real one. The 1D model does not allow to calculate the low frequency pressure pulsation.

The DSF pressure pulsation amplitudes Δp_{2f} calculated over the 2D model are in 3–4 times higher than the experimental ones (Table 1), but still closer to the experiment than calculated over the 1D model.

The electromagnetic pressure Δp_{em} was calculated by integrating the x-component of the electromagnetic force over the entire calculation region.

Table 1. Comparison of some calculated and experimental ALIP characteristics.

Slip,	Δp, 10^5 Pa			$\delta p_{\rm low}/\delta p_{em}$		$\delta p_{2f}/\delta p_{em}$		
s	Exp-nt	1D mod.	2D mod.	Exp-nt	2D mod.	Exp-nt	1D mod.	2D mod.
0.47	2.12	2.42	2.19			0.03	0.125	0.076
0.72	2.78	2.99	2.94	0.05	0.012	0.02	0.127	0.050
0.78	2.87	3.14	3.12	0.05	0.059	0.01	0.123	0.036

3. Conclusion. (1) The 2D model to analyze the MHD instability in an ALIP has been developed and tested. The numerically obtained flow patterns are presented for uniform ($\mathrm{Rm}\, s < \mathrm{Rm}_{\rm crit}$), and non-uniform ($\mathrm{Rm}\, s > \mathrm{Rm}_{\rm crit}$) types of the flow, the latter being characterized by large vortices, moving in axial and azimuthal directions. For the ALIP-2, $\mathrm{Rm}_{\rm crit} \approx 1.4$ according to calculations and $\mathrm{Rm}_{\rm crit} \approx 1.3 - 1.4$ in the experiments. (2) The 2D model demonstrates good qualitative and satisfactory quantitative agreement with the experimental results.

REFERENCES

1. Y.A. Polovko *et al.* *Journal of Techn. Phys.*, vol. 66 (1996), no. 4, pp. 36–44. (in Russ).
2. Y.A. Polovko *et al.* *Journal of Techn. Phys.*, vol. 67 (1997), no. 6, pp. 5–9. (in Russ).
3. Y.A. Polovko *et al.* In *Proc. the Third Intern. Conf. on Transfer Phenomena in MHD and Electroconducting Flow* (Aussois, France, 1997), vol. 2, p. 451.
4. I.R. Kirillov *et al.* *Magnetohydrodynamics*, vol. 16 (1980), no. 2, p. 196.
5. I.R. Kirillov, V.P. Ostapenko. *Magnetohydrodynamics*, vol. 23 (1987), no. 2, pp. 196–202.
6. H. Araseki *et al.* *Nuclear Engineering and Design*, vol. 227 (2004), p. 29.
7. R.A. Valdmane *et al.* *Magnetohydrodynamics*, vol. 18 (1982), no. 3, p. 293.
8. I.R. Kirillov, D.M. Obukhov. *Energy Conversation and Management*, vol. 44 (2003), pp. 2687–2697.